Geochemistry and Petrogenetic Evolution of Rocks around Bishewa-Ologomo area, part of Lafiagi Sheet 203, Northcentral Nigeria.

Jimoh Ajadi

Abstract – Geochemical analysis of rock samples from Bishewa-Ologomo area was carried out for oxides of major and trace elements including rare earth using the XRF analytical method. The granitic rocks of the area are interpreted as being formed by partial melting due to its high LREE / HREE ratios and the presence of slight negative Eu anomalies. The result shows that the granites of this area are primarily of igneous source, but with possible sedimentary input during emplacement. The Rb versus Y+Nb, Nb versus Y and Rb versus SiO_2 discrimination plots suggest that the evolution of the granitic rocks of the study area ranges from syn-collisional to volcanic arc origin. The high P_2O_5 values varying between 0.2%-0.57% for granodiorite, medium-grained biotite granite, quartz-mica schist and medium-coarse grained biotite-hornblende granite of the area are well above apatite saturation level of 0.14% [12] which can be correlated with progressive enrichment of the lighter REE (La – Sm) in the fractionating magma. All the metasediments of the area plot within the sedimentary field. The TiO_2-K_2O-P_2O_5 molecular discrimination diagram shows the mafic rocks of the study area are of the tholeiitic oceanic basalt origin.

KEYWORDS: Geochemistry, Analysis, Petrogenesis, Tectonic Deformation, Structural Evolution, Discrimination plot, Bishewa-Ologomo.

1 INTRODUCTION

Field observations and geochemical studies on the rocks of the Bishewa-Ologomo areas were carried out to determine the geochemistry and petrogenesis of the subsurface geology. The data obtained was interpreted with a view to understanding the petrogenetic evolution and reconstruct the geological history of the study area. The area lies within the crystalline Precambrian Basement Complex of Nigeria with rocks bearing the imprints of the N-S structural trends that are frequently associated with the Nigeria Basement Complex rocks. The migmatite gneiss complex is the oldest basement rock and it is believed to be of Archaean age [4]. Some authors have described the basement complex rocks of Nigeria as a heterogeneous rock assemblage, which include migmatites, paragneisses, orthogneisses, quartzites, paraschists and a series of basic to ultrabasic metamorphosed rocks [11]. Field evidence shows that the study area has suffered from polyphase tectonic deformations with associated igneous activities. Rocks outcropping in Bishewa-Ologomo area form part of the northern limit of the migmatite-gneiss complex in the Southwestern sector of the Nigerian Basement unconformably overlain by the sediments of the Bida basin in the northeastern part of the study area. The study area, which covers part of Lafiagi and Ifelodun local government areas in Kwara state, is located in the northwestern sector of the Lafiagi Southwest (sheet 203 – 1:50,000) and bounded by latitudes 8°39' N to 8°46' N, and longitudes 5°03'E to 5°11'E (Fig. 1).

- *Jimoh Ajadi is currently pursuing Ph.D. degree program in Geology in the Department of Chemical, Geological and Physical Sciences at the Kwara State University, Malete, P.M.B. 1530, Ilorin, Nigeria.*

E-mail: jimoh.ajadi@kwasu.edu.ng, jimohajadi@gmail.com, Telephone: +234(0)8136436333

2 GEOLOGY OF BISHEWA-OLOGOMO AREA

Four major lithological groups were mapped in the study area. These include the biotite gneiss and migmatitic gneiss as the early metamorphic tectonites. A U/Pb age was obtained on a zircon fraction extracted from an orthogneiss in Kaduna to be Early Archaean (>3.05Ga), while the age of emplacement and crystallization of the original granodiorite prior to its deformation was put at >3.65Ga [2]. Other authors who worked on Nigerian migmatites also obtained similar Archaean ages [5][6]. The biotite schist, quartz-mica schist, quartzite and amphibolite, which is being partly altered to talc-tremolite schist, constitute the metasedimentary rocks. The felsic rocks are composed of the porphyritic granite, granodiorite, medium-grained granite, medium-coarse grained biotite granite, leucogranite, pegmatite, aplite and quartz veins, while the hornblende-quartz diorite, porphyritic diorite and lamprophyre form the un-metamorphosed mafic rocks.

The two major varieties of schist comprising quartz-muscovite schist and quartz-biotite schist which are believed to have resulted from the considerably varied alteration and replacement products of the constituent minerals particularly biotite and feldspar constitute the most widespread rocks forming extensive background to other rocks in the area. Differential erosion features which resulted from the removal of easily weathered schist leave the associated intrusives as small resistant ridges that characterize the schist belt. The discontinuous bands of amphibolite weathers down and sometimes locally grades into pockets of tremolite-talc schist with characteristic soapy feel.

A band of N-S trending foliated quartzite was mapped some 2km southwest of Ologomo in the south central part of the study area. The quartzite mostly occurs in rubbles and cobbles of angular quartzite blocks and boulders. Amphibolite occurs as thin concordant bands and lenses trending NNW-SSE and dipping moderately easterly. The rock is medium- to coarse-grained with occasional porphyroblasts of hornblende. Rocks of the gneiss-migmatite-schist complex are predominant around the study area and are intruded by syn- to post-tectonic granitic and pegmatitic rocks of probable Pan African age.

Minor intrusives include lamprophyre, diorite, pegmatite, aplite and vein quartz and are observed as veins, bosses and dykes of limited aerial extent. A thick pile of sedimentary rocks, which forms an integral part of the southern flank of the Bida basin, underlies a portion of the northeastern part of the study area. The sedimentary/basement contact is observable in the northern outskirt of Bishewa where it is marked by basal intraformational conglomerates (Fig. 2).

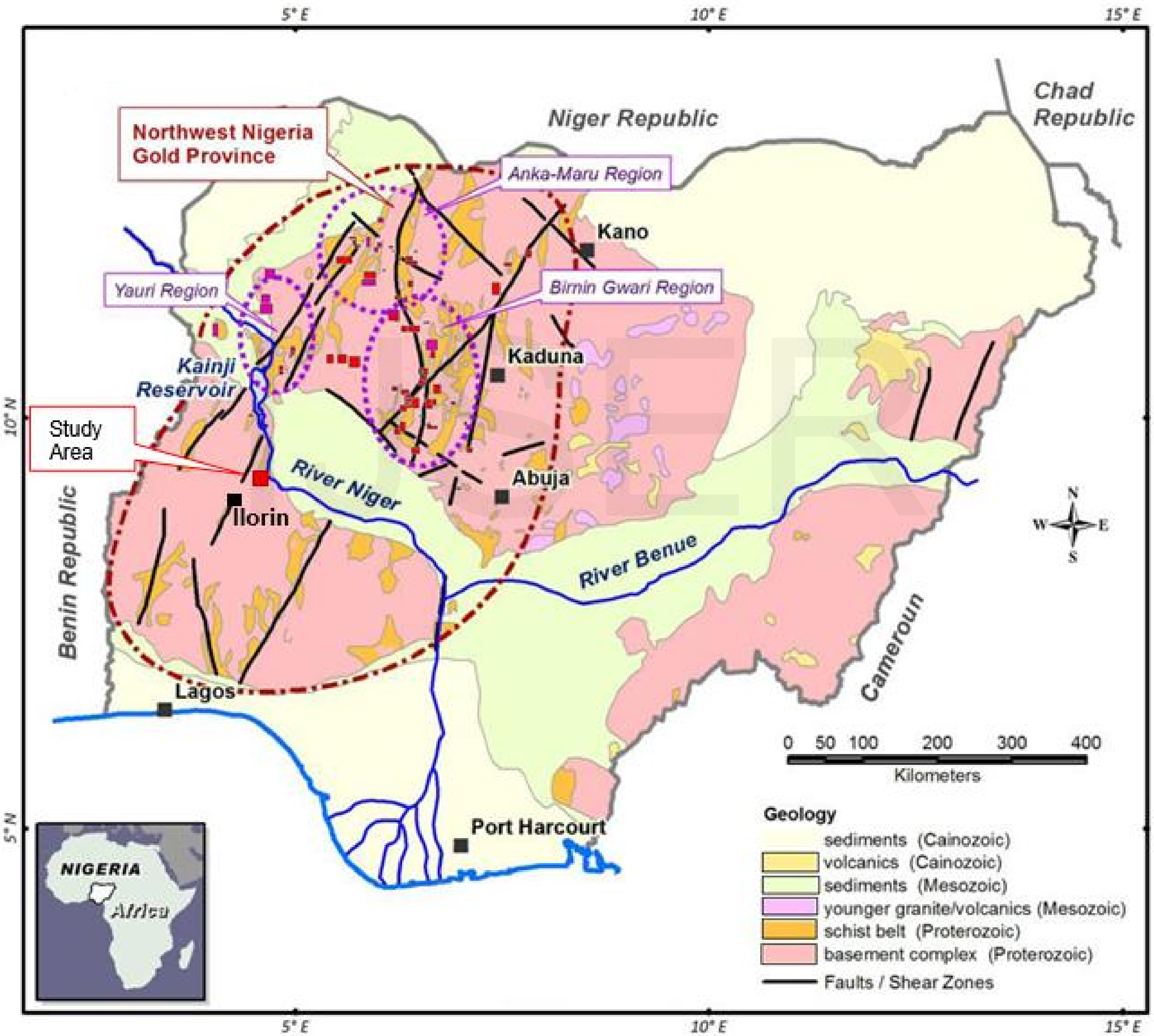

Fig. 1: Generalized geological map of Nigeria showing the study area (modified from [9]).

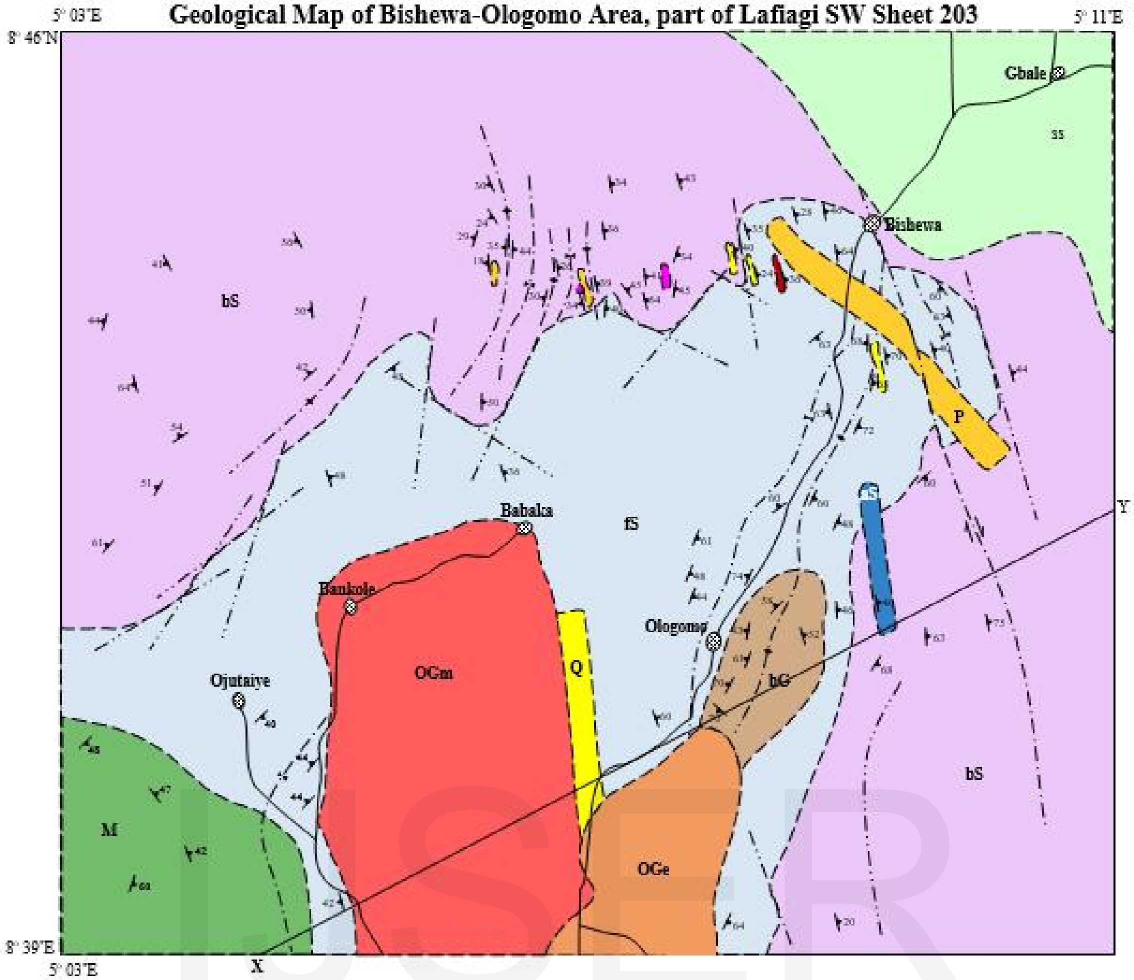

Fig. 2: Geological map of Bishewa-Ologomo area showing liuthological distribution (modified after [1])

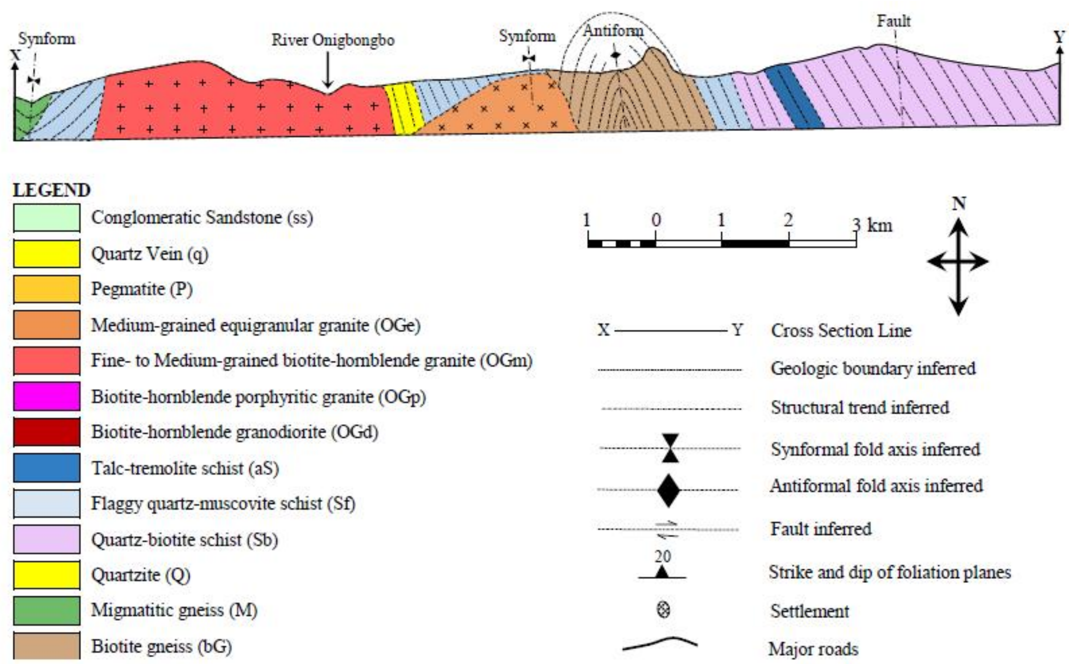

3 FIELD OBSERVATIONS AND STRUCTURAL ANALYSIS

About three (3) main deformational episodes have been recorded in the study area. The first episode of structural deformation (D_1) in the area probably produced the primary metamorphic fabrics represented by the lithological and mineralogical banding (S_0,S_1), which changed the physico-chemical structure of the sedimentary precursor. This is largely observable only in areas of tectonic shadows.

The second major tectonic deformation (D_2) affected the S_0,S_1 surfaces and folded it into tight isoclinal folds (F_1) thereby producing the S_2 surfaces, which are axial planar to F_1. This is particularly evident on few outcrops of the biotite and migmatitic gneisses where a superimposition of a later axial planar cleavage (S_2) on an earlier planar fabric (S_0,S_1) was observed (Fig. 3). Generally, S_1 trends NW-SE dipping northeasterly while the S_2 foliation plane, which is the pervasive planar fabric in the study area trends mostly NE-SW dipping either southeasterly or northwesterly.

The third and possibly the last major episode of tectonic deformations (D_3) are observable in some localities where the D_3 deformation refolded the S_2 surfaces resulting in the formation of major folds (F_2) (Fig. 4), which are sometimes recumbent (Fig. 5) and plunging, upright, open or close. D_3 is also perhaps responsible for the formation of the inferred regional fold and several fractures including joints, shears and faults mapped in the study area.

4 LABORATORY PROCEDURE

Sixteen (16) representative samples of the lithologies mapped in the study area were analyzed using the XRF method for oxides of major and trace elements, including rare earth elements at the Activation Laboratory in Canada. These samples were prepared for chemical analysis by crushing and reducing it to 1mm size using a Geocrusher and pulverizer. 200g of samples were ground to –200 mesh using a disc mill. Sample contamination was prevented by carrying out air cleaning at each stage. Hot digestion of 0.5g of the sample in a mixture of HNO_3, $HClO_3$ and HF was carried out before the XRF analysis to determine the chemical composition of the 16 selected samples.

5 RESULTS AND INTERPRETATION

The chemical compositions in terms of major, trace and rare earth elements data for the 16 whole rock samples are presented in Tables 1, 2 and 3. The result shows that the porphyritic granite, pegmatite and medium-coarse grained biotite-hornblende granite are silica saturated with values ranging between 71.98% – 73.36%. Metasediments such as the biotite-hornblende schist and biotite gneiss are also silica saturated varying from 74.06% – 75.51. Al_2O_3 is consistently high in all the whole rock sampled, ranging between 10.22% and 21.31%, indicating that all samples are corundum normative.

Rocks such as granodiorite, lamprophyre, quartz diorite, medium-grained granite, amphibolite and tremolite/talc schist show greater enrichments in cafemic oxides (CaO, Fe_2O_3, MgO), which varies from 4.38% – 20.26%, 6.54% – 10.54% and 2.25% – 22.08% respectively. The variation in the cafemic oxides composition is due to differences in the high percentage content of amphibolite, biotite and sphene in these rocks.

The general classification plot [3] for the volcanic and plutonic rocks of the study area (Fig. 6) shows that the felsic rocks including pegmatite, porphyritic granite and granodiorite are rhyolitic, the mafic rocks comprising medium grained granite and quartz diorite are trachy-andesite while amphibolite and porphyritic diorite are basaltic in composition. The classification plot of FeO_{total}/MgO_{total} versus SiO_2 [8] also shows that the amphibolite is tholeiitic in composition (Fig. 7).

The discrimination plots [10] (Figs. 8, 9 and 10) indicates that the porphyritic granite and pegmatites of the study area are syn-collisional in origin while the quartz diorite, porphyritic diorite, granodiorite and medium-grained granite are of volcanic arc origin. The discrininattion plot of Na_2O/Al_2O_3 versus K_2O/Al_2O_3 [7] for the igneous and metasedimentary rocks of Bishewa-Ologomo area (Fig. 11) revealed that the lamprophyre, pegmatite, porphyritic granite are of igneous origin. Other rocks of the study area including the muscovite schist, biotite schist, amphibolite, quartzite, biotite gneiss as well as the porphyritic diorite, quartz diorite, granodiorite and medium grained granite fall within the sedimentary field.

Rocks of the Bishewa-Ologomo area show a slightly increase in LREE (La-Sm)/HREE (Eu-Lu) ratios and a low negative Eu anomalies on the chondrite-normalized REE plot, which suggests a possible sedimentary origin for the Older Granite suites of the study area with possible igneous contribution. This is consistent with the plot of the ratios of Na_2O/Al_2O_3 versus K_2O/Al_2O_3 for the discrimination of igneous and sedimentary/metasedimentary rocks [7], which shows the rocks of the study area plotting well within sedimentary field.

These, therefore, indicates a REE fractionation pattern derived primarily from a sedimentary source with significant contamination from residual hornblende, clinopyroxene and garnet in a host source rock of igneous origin. Rocks of tonalitic to granodioritic composition with negative Eu anomalies and high LREE/HREE ratios have been interpreted by some authors [13] as primary melt derived by partial melting of a mafic gneiss or amphibolite containing some combination of hornblende, garnet, clinopyroxene and plagioclase. This can be interpreted as being suggestive of the presence of hornblende and/or apatite left in the residue after partial melting of a mafic source rock.

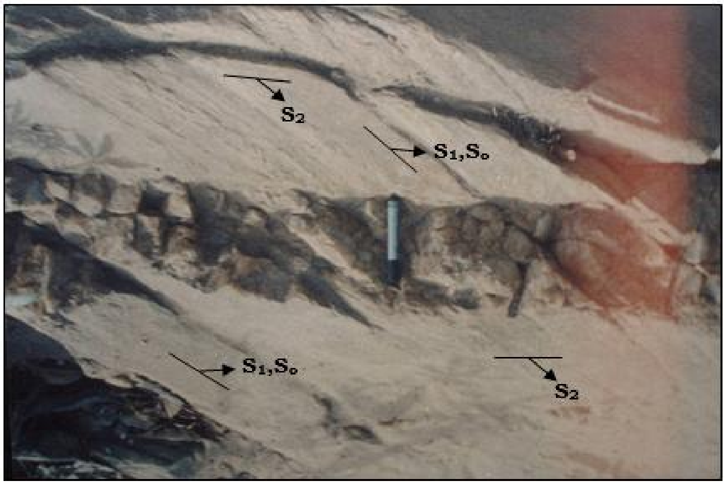

Fig. 3: Outcrop of biotite gneiss showing the axial planar cleavage foliation plane (S_2) superimposed on relict lithologic foliation plane (S_1,S_o) formed from pelitic bands of sedimentary origin.

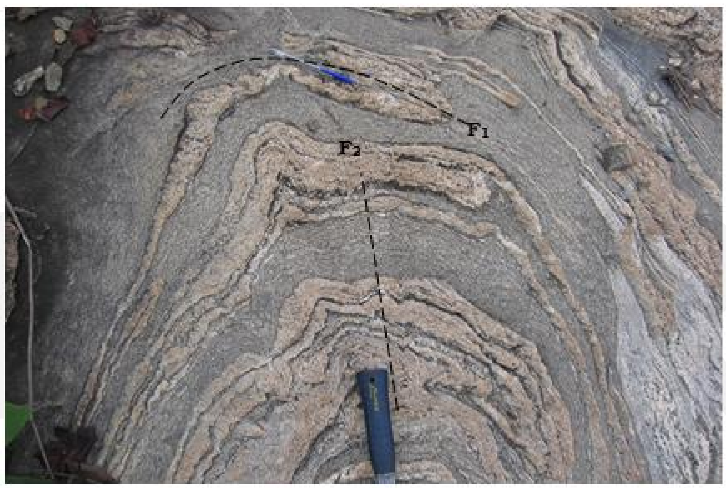

Fig. 4: Polyphase folding systems in migmatitic gneiss with at least two episodes of folding which Produced the tight isoclinal fold (F_1) and an upright fold (F_2) with crenulations on the closure of the F_2 fold.

Fig. 5: A recumbent fold in a pegmatized quartz-biotite schist.

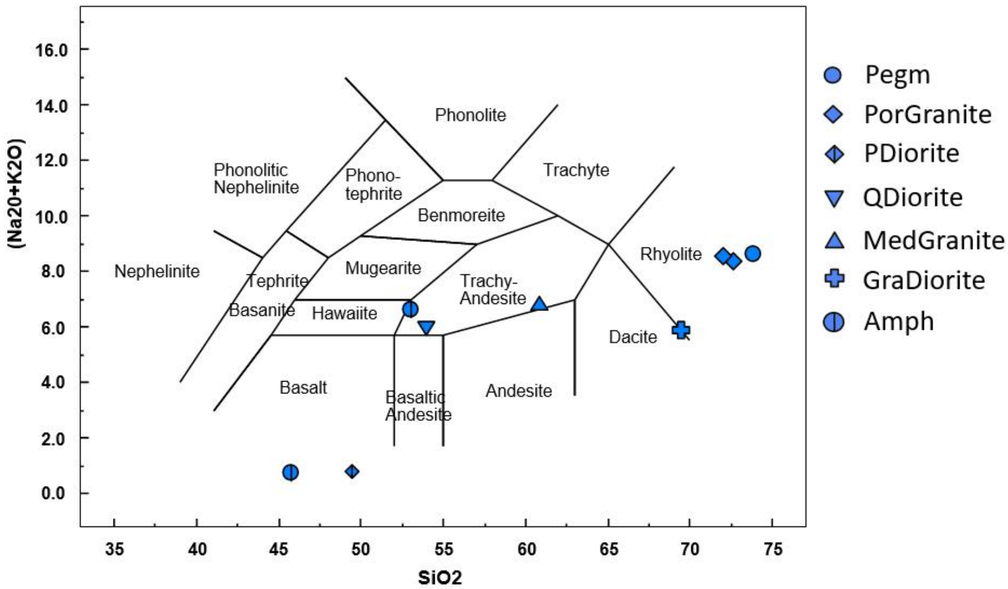

Fig. 6: TAS Alkalis-Silica plots [3] for volcanic and plutonic rocks of Bishewa-Ologomo area.

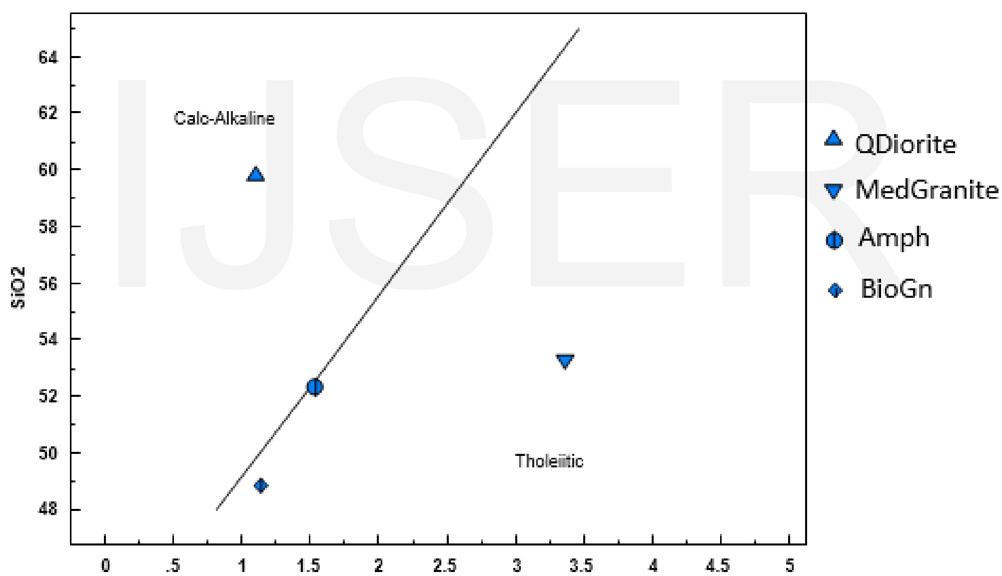

Fig. 7: The FeO_{total} / MgO_{total} versus SiO_2 general classification plot [8].

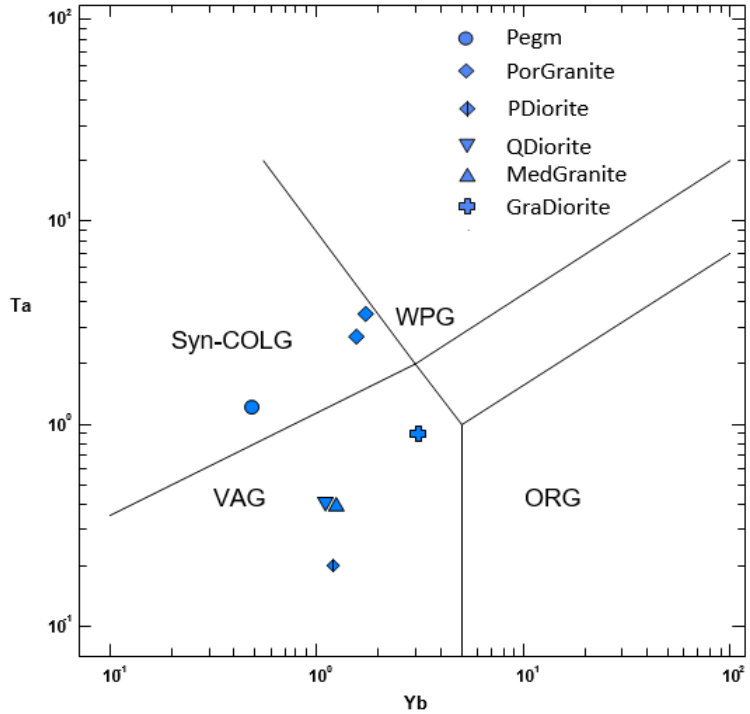

Fig. 8: Log (Ta) versus Log (Yb) for granites of the study area [10].

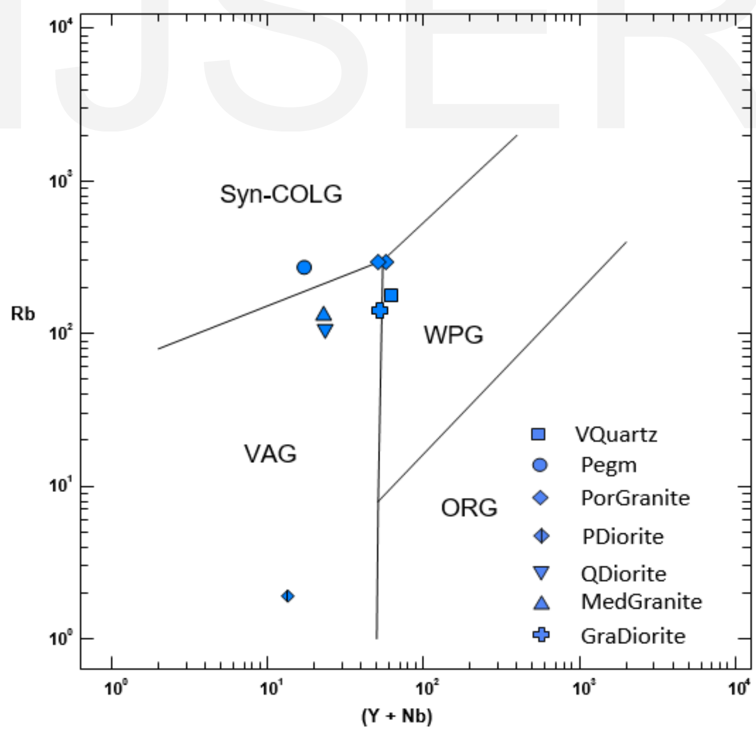

Fig. 9: Log (Rb) versus Log (Y+Nb) for granites of the study area [10].

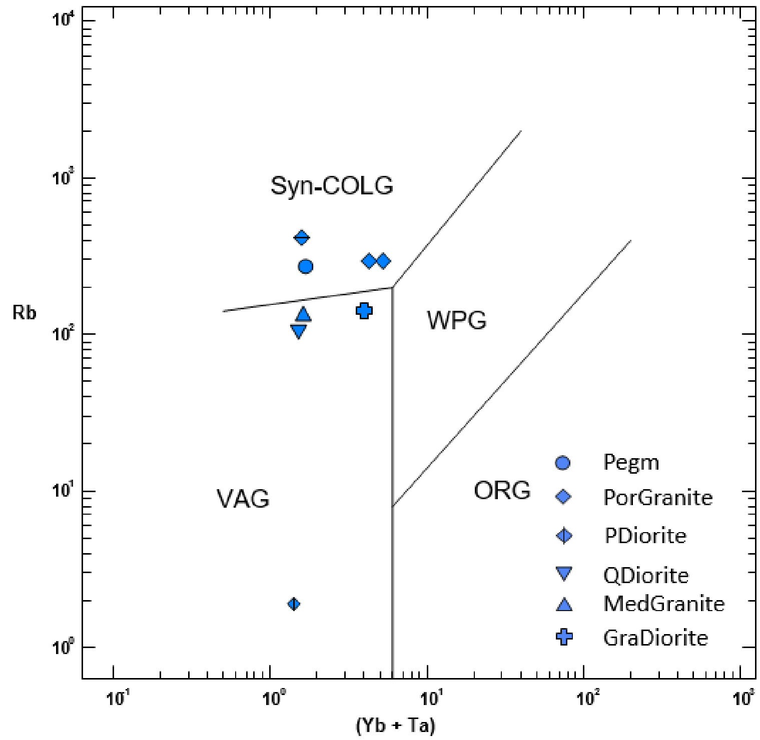

Fig. 10: Log (Rb) versus Log (Yb+Ta) for granites of the study area [10].

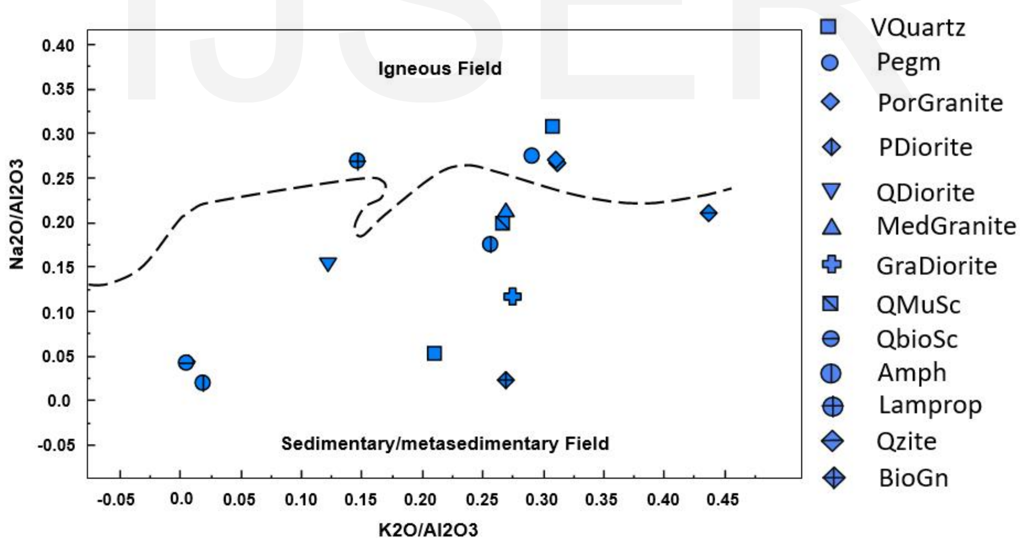

Fig. 11: Na_2O / Al_2O_3 versus K_2O / Al_2O_3 plot of Igneous and metasedimentary rocks of Bishewa / Ologomo area (Adapted from [7]).

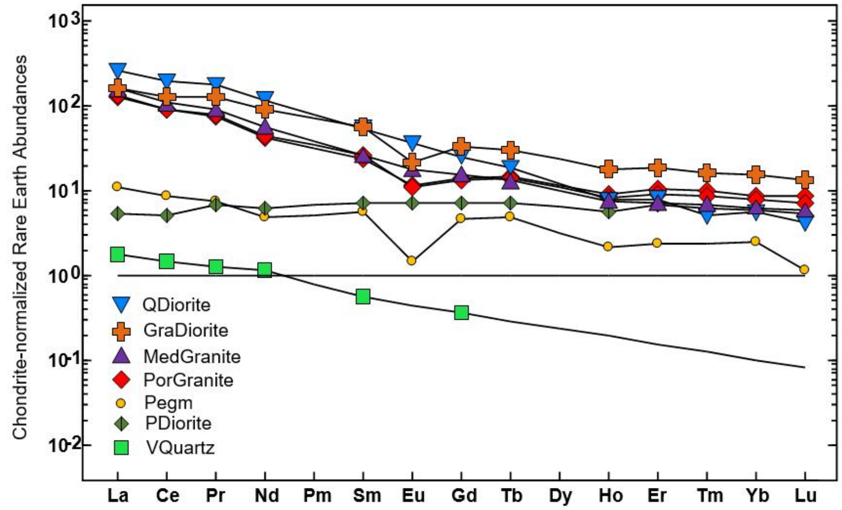

Fig. 12: Chondrite-normalized REE composition for the granitic rocks of Bishewa-Ologomo area.

Table 1: Chemical Analysis of the Major Element Oxides of some samples (%)

Element	SiO_2	Al_2O_3	Fe_2O_3	MgO	CaO	Na_2O	K_2O	TiO_2	P_2O_5	MnO	Cr_2O_3	Sc	LOI	TOT/C	TOT/S	SUM
Samples	%	%	%	%	%	%	%	%	%	%	%	ppm	%	%	%	%
VQuartz	98.62	0.19	0.78	0.01	<.01	0.01	0.04	<.01	0.03	<.01	<.001	<1	0.1	0.02	<.01	99.78
SmoQuartz	98.13	0.13	0.69	0.01	0.02	0.04	0.04	<.01	0.03	<.01	<.001	<1	0.7	0.02	<.01	99.78
Pegm	73.36	15.12	1.19	0.15	0.58	4.14	4.4	0.04	0.2	0.05	<.001	2	0.5	0.03	<.01	99.73
PorGranite1	71.98	14.29	2.23	0.4	1.48	3.8	4.46	0.29	0.1	0.06	<.001	4	0.5	0.05	<.01	99.59
PorGranite2	71.16	14.53	2.26	0.39	1.54	3.93	4.52	0.25	0.1	0.06	<.001	4	0.7	0.06	<.01	99.44
PDiorite	48.84	15.25	10.08	8.83	14.16	0.66	0.11	0.61	0.05	0.17	0.04	47	1	0.06	0.01	99.82
QDiorite	53.2	21.31	7.59	2.25	6.8	3.24	2.61	0.81	0.57	0.06	<.001	6	0.8	0.04	0.15	99.23
MedGranite	59.9	13.88	6.54	5.92	4.38	2.97	3.75	0.66	0.23	0.09	0.091	13	1.1	0.13	0.2	99.53
GraDiorite	68.66	14.74	5.22	1.35	2.14	1.71	4.05	0.62	0.2	0.09	0.003	10	1.1	0.02	<.01	99.89
QMuSc	74.06	12.67	3.33	0.74	2.27	2.52	3.38	0.45	0.15	0.05	0.002	9	0.2	0.02	0.01	99.82
QbioSc	44.5	10.22	10.54	22.08	6.17	0.42	0.06	0.14	0.02	0.17	0.568	26	4.8	0.03	<.01	99.82
Amph1	45.04	17.97	8.44	3.83	20.26	0.32	0.36	1.93	0.12	0.15	0.006	18	0.9	0.08	0.09	99.33
Amph2	52.3	15.06	9.48	6.14	7.47	2.61	3.88	1.04	0.46	0.15	0.027	30	0.9	0.03	0.26	99.53
Lamprop	75.51	12.62	2.77	0.89	1.65	3.38	1.86	0.37	0.11	0.04	0.002	8	0.7	0.02	0.01	99.9
Qzite	72.77	15.11	0.74	0.08	0.28	3.16	6.61	0.01	0.14	0.01	<.001	1	0.7	0.01	<.01	99.61
BioGn	94.3	3.27	0.68	0.05	<.01	0.07	0.88	0.16	0.02	0.01	0.002	1	0.3	0.02	0.01	99.74

Table 2: Chemical Analysis of the Rare Earth Elements of some selected samples (ppm)

Element	La	Ce	Pr	Nd	Sm	Eu	Gd	Tb	Dy	Ho	Er	Tm	Yb	Lu
SAMPLES	ppm	ppm	ppm	ppm	ppm	ppm	ppm	ppm	ppm	ppm	ppm	ppm	ppm	ppm
VQuartz	0.6	1.3	0.14	0.7	0.1	<.05	0.09	<.01	<.05	<.05	<.05	<.05	<.05	<.01
SmoQuartz	<.5	<.5	<.02	<.4	<.1	<.05	<.05	<.01	<.05	<.05	<.05	<.05	<.05	<.01
Pegm	3.6	7.8	0.86	2.9	1	0.1	1.13	0.23	1.34	0.15	0.48	<.05	0.49	0.04
PorGranite1	42	78.2	8.21	25.4	4.2	0.81	3.44	0.68	3.55	0.64	2.13	0.3	1.74	0.29
PorGranite2	43.8	80.5	8.61	26.9	4.8	0.77	3.34	0.65	3.07	0.59	1.79	0.26	1.55	0.24
PDiorite	1.8	4.5	0.75	3.8	1.3	0.49	1.74	0.34	2.07	0.39	1.38	0.19	1.2	0.18
QDiorite	84.7	170.1	19.8	70	9.8	2.49	6.25	0.88	3.78	0.54	1.59	0.15	1.11	0.14
MedGranite	52.3	95.9	10.23	34.5	4.7	1.23	3.9	0.62	3.03	0.53	1.45	0.2	1.24	0.2
GraDiorite	53.4	113.6	14.53	53.7	10	1.46	8.36	1.43	7.39	1.26	3.79	0.48	3.09	0.46
QMuSc	23.7	59.2	6.68	24.8	5.5	0.77	5.83	1.3	7.88	1.56	4.88	0.67	4.39	0.7
QbioSc	3.6	5.3	0.88	3	0.7	0.15	0.79	0.13	1.27	0.23	1.04	0.1	0.99	0.13
Amph1	18.2	38.7	4.44	16.5	3	1.57	2.09	0.35	1.81	0.33	1.11	0.18	1.17	0.2
Amph2	35.4	74.3	8.96	36	6.6	1.83	5.97	1.01	5.29	0.94	2.85	0.37	2.55	0.39
Lamprop	25.3	51.5	5.71	20.5	3.9	0.72	4.27	0.89	5.33	1.04	3.23	0.4	2.46	0.34
Qzite	1.1	1.7	0.15	0.4	0.2	0.06	0.23	0.04	0.42	<.05	0.23	<.05	0.28	0.01
BioGn	4.6	7.8	0.82	2.9	0.5	0.2	0.55	0.08	0.88	0.18	0.74	0.07	0.77	0.1

Table 3: Chemical Analysis of the Trace Elements of some samples

Element	Ba	Be	Co	Cs	Ga	Hf	Nb	Rb	Sn	Sr	Ta	Th	U	V	W
Sample	ppm	ppm	ppm	ppm	ppm	ppm	ppm	ppm	ppm	ppm	ppm	ppm	ppm	ppm	ppm
VQuartz	6.6	<1	0.9	0.1	<.5	<.5	<.5	1.8	1	2.2	<.1	0.1	<.1	<5	0.4
SmoQuartz	0.7	2	1.1	0.1	<.5	<.5	<.5	2	1	1.1	0.4	<.1	<.1	<5	0.1
Pegm	78	7	0.6	12.6	18.7	1.3	9.8	267.5	17	22.7	1.2	1.4	2.9	<5	1
PorGranite1	490.8	13	3.6	21.6	23.6	4.6	36.9	293.9	5	236.1	3.5	22.1	11.7	19	0.8
PorGranite2	476.5	13	2.9	20.8	23.8	4.8	30.9	296	5	242.4	2.7	22.6	8.2	17	0.7
PDiorite	93.9	<1	40.3	0.2	13	0.8	1.4	1.9	2	89.7	0.2	<.1	<.1	244	10.5
QDiorite	2991.5	2	13.7	8.4	22.9	3.4	6.8	104	1	2104.6	0.4	11.4	1.4	95	0.5
MedGranite	1328.4	2	28.6	3.9	19	5.7	7.4	135.9	2	455.3	0.4	9.5	1	97	0.5
GraDiorite	704.9	<1	10.3	2.1	16.4	5.6	13.3	140.7	3	123	0.9	13.7	1	53	2.4
QMuSc	417	1	5.6	16.6	13.4	4.9	13.9	175.8	4	83.1	1.2	1.7	0.8	49	1
QbioSc	9.9	1	94	0.1	6.8	<.5	0.6	0.7	<1	7.8	0.1	0.7	0.1	107	0.1
Amph1	111.6	2	25.8	3	28	15.1	21.1	13.7	3	898.1	0.9	3.1	0.6	181	2.2
Amph2	1759.4	2	34.4	1	17.3	4.6	11	103.1	3	397.3	0.5	4.5	1	199	26.4
Lamprop	599.2	18	5.1	61.4	12.7	4.7	4.7	495.4	5	72.6	0.2	0.5	0.8	37	2.4
Qzite	35	4	0.6	10.1	12.4	0.8	7.2	405.9	6	32.2	1.3	0.2	3	<5	0.9
BioGn	158.8	<1	0.7	0.6	2.6	8.3	2.1	27.8	1	16.1	0.2	0.8	0.4	8	1.5

Table 3 continued. Chemical Analysis of the Trace Elements of some samples

Element	Zr	Y	Mo	Cu	Pb	Zn	Ni	As	Cd	Sb	Bi	Ag	Au	Hg	Tl	Se
Sample	ppm	ppm	ppm	ppm	ppm	ppm	ppm	ppm	ppm	ppm	ppm	ppm	ppb	ppm	ppm	ppm
VQuartz	1.9	0.3	1.1	9.4	0.2	1237	5.1	1.7	0.2	0.2	<.1	<.1	1.3	<.01	<.1	<.5
SmoQuartz	1.7	<.1	1.4	13.4	0.1	2464	7.3	2	0.5	0.2	<.1	<.1	1.3	<.01	0.1	<.5
Pegm	28.1	7.4	0.5	5.4	1.8	1341	2.2	0.9	0.4	0.1	0.1	<.1	<.5	<.01	<.1	<.5
PorGranite1	136.3	20.9	0.4	10.1	3.8	2657	4.7	1.3	3.8	0.1	0.1	<.1	1.8	<.01	0.5	<.5
PorGranite2	164.4	20	0.5	9.7	3.9	2725	4.8	1.2	3.6	0.1	0.1	<.1	0.8	<.01	0.5	<.5
PDiorite	23.4	12.2	0.8	50.5	2.6	561	10.1	2	0.1	0.1	<.1	<.1	1.7	<.01	0.1	<.5
QDiorite	142.2	16.6	0.8	16.9	2.2	435	4.6	1.3	0.1	0.1	0.1	<.1	<.5	<.01	0.5	<.5
MedGranite	203.6	15.6	0.5	22.4	3.5	2161	121.7	1.1	0.3	0.1	<.1	<.1	2.2	<.01	0.6	<.5
GraDiorite	202.2	39.4	0.4	9.4	2.2	310	13.5	0.8	0.1	0.2	<.1	<.1	<.5	<.01	0.4	<.5
QMuSc	157.9	47.4	0.4	4.5	0.5	1179	5.2	1.3	0.3	0.1	0.1	<.1	<.5	<.01	0.6	<.5
QbioSc	13.7	8.7	0.2	5	0.3	643	236.8	0.5	6.2	0.1	<.1	<.1	0.8	<.01	<.1	<.5
Amph1	597.5	10.4	0.3	25.2	3.5	3003	13.3	1.5	0.8	0.1	<.1	<.1	<.5	<.01	<.1	<.5
Amph2	174	27.8	0.7	111.3	5.2	656	29	1.3	0.1	<.1	0.1	0.1	2.1	<.01	0.3	0.5
Lamprop	156.4	29.9	0.4	3.9	0.5	531	7.4	0.8	0.2	0.1	<.1	<.1	0.9	<.01	2.6	<.5
Qzite	20	3	0.4	7.3	2.7	2391	2.2	1.1	0.6	0.1	0.1	<.1	<.5	<.01	<.1	<.5
BioGn	310.3	6.4	0.8	8.4	0.3	1070	3.5	1.3	0.2	0.1	<.1	<.1	0.8	<.01	<.1	<.5

6 DISCUSSION

Information derived from field observations, thin section studies and geochemical analysis reveal that the geological history of the study area involves the biotite-hornblende gneiss and the migmatitic gneiss as the earliest metamorphic tectonites in this area. The migmatite gneiss complex is the oldest basement rock and it is believed to be of Archaean age [4]. A period of hiatus followed, which corresponds to a time of orogenic activities, metamorphism and reactivation of pre-existing rocks. The migmatitic gneiss forms the crystalline basement on which the deposition of arenites in N-S trending basins took place in the Birrimian. Another period of non-deposition followed during the Eburnean orogeny, which metamorphosed and deformed the schist belts along with the enclosing basement. The arenites were variously metamorphosed to form the different rocks of the schist belt. The emplacement of the Older Granite suites followed in the Pan-Africa.

The granite emplacement took place in the Pan-African time (600 to 700 Ma). This was accompanied by the emplacement of the late-stage intrusions such as quartz-hornblende diorite, pegmatite, aplite and vein quartz at the waning stage of the Pan-African event. In the Mid-Cambrian, another period of hiatus took place accompanied by epeirogenic uplift, fracturing and high-level magmatic activities. The period of hiatus was interrupted by the deposition of a thick pile of sedimentary rocks, which forms the Cretaceous Bida basin. Erosion and uplift followed and was capped by the deposition of clastic sediments of post Cretaceous to Recent alluvial sand deposits. This continues, though slowly, shaping and changing the topography of the study area.

7 CONCLUSION

Field and petrographic data have shown that the Basement Complex rocks underlie the study area, which has been affected by series of polycyclic deformations that affected the southwestern sector of the Nigerian Basement Complex. The granitic rocks of the study area, based on geochemical data, can be interpreted to have been formed from a sedimentary precursor by partial melting with possible igneous input during emplacement, which is evident in its low LREE/HREE ratios and minimal Eu anomalies. The Rb versus Y+Nb, Rb versus Yb+Ta and Ta Versus Yb discrimination plots suggest that the evolution of the granitic rocks of the study area ranges from syn-collisional to volcanic arc origin.

The weak Eu negative anomalies on the chondrite-normalized REE plots for the granites may be suggestive of the presence of hornblende and / or apatite left in the residue after partial melting of a mafic sedimentary source rock. The high P_2O_5 values varying between 0.2%-0.57% for granodiorite, medium-grained biotite granite, quartz-mica schist and medium-coarse grained biotite-hornblende granite of the area are well above apatite saturation level of 0.14%. This correlates with the weakly enriched lighter REE (La – Sm) in the fractionating magma. The molecular discrimination diagram shows the mafic rocks of the study area are of the tholeiitic basalt origin.

REFERENCES

[1] Adekeye J. I. D, Ajadi J., Adedoyin A. D., Bamigboye O. S. and Alabi A. G. F. (2015). Origin and Structural Control of Gold Mineralization in Bishewa Area, Central Nigeria. In Centrepoint Journal, University of Ilorin Nigeria (Sci. Ed.) Vol. 21 (1) pp. 13-34.

[2] Bruguier O., Dada S. S. and Lancelot J. R. (1994). Early Archaean component (>3.5Ga) within a 3.05Ga orthogneiss from Northern Nigeria: U-Pb zircon evidence. Earth and Planetary Science Letters 125, pp. 89-103.

[3] Cox, K. G., Bell, J. D., & Pankhurst, R. J., 1979. The Interpretation of Igneous Rocks. London: Allen & Unwin.

[4] Dada, S.S. (1989) Evolution de la croute continental au Nord Nigeria: apport de la geochimie, dela geochronologie U-Pb et des traceurs isotopiques Sr, Nd et Pb. Ph.D. Thesis University of Science and Technology Languedoc, Montpellier, France.

[5] Dada S. S. (1998). Crust-forming ages and proterozoic crustal evolution in Nigeria: a reappraisal of current interpretations. Precambrian Research 87, pp. 65-74.

[6] Ekwuewe B. N. (1991). The Geology of the Area around Obudu Cattle Ranch, S.E. Nigeria. Journal of Min. Geology (1), pp. 129-134.

[7] Garrels, R.M. and Mackenzie, F.T. (1971). Evolution of sedimentary rocks. W. W. Norton (Ed), New York, 394p.

[8] Miyashiro A. (1974). Volcanic rock series in island arcs and active continental margins. American Journal of Science 274, pp. 321–355.

[9] Neil Warburton and Dominic Marinelli (2011). Report of the Australian Mines Limited on Acquisition of Nigerian Gold Properties Limited.

[10] Pearce, J. A., Harris, N. B. W. and Tindle, A. G. (1984). Trace element discrimination diagrams for the tectonic interpretation of granitic rocks. Jour. Petrol. 25, pp. 956-983.

[11] Rahaman, M.A. (1988). Recent advances in the study of the Basement Complex of Nigeria. In Precamb. Geol. of Nigeria, (Oluyide, P. O., Mbonu, W. C., Ogezi, A. E., Egbuniwe, I. G. Ajibade, A. C. and Umeji, A. C. Eds.), G. S. N. Report, pp. 11-41.

[12] Watson, E. B. and Capobianco, C. J. (1981). Phosphorus and the rare earth elements in felsic magmas: an assessment of the role of apatite. Geochim. Cosmochim. Acta, 45, pp. 2349-2358.

[13] Witt, W. K. and Swager, C. P. (1989). Structural setting and geochemistry of Archean I-Type granites in the Bardoc-Coolgardie area of the Norseman-Wiluna belt, West Australia. Precamb. Res. 44, pp. 323-351.